Faraday Discussions

Accepted Manuscript

Faraday Discussions

Royal Society of Chemistry

ROYAL SOCIETY OF CHEMISTRY

www.rsc.org/faraday_d

Modelling component evaporation and composition change of traffic-induced ultrafine particles during travel from street canyon to urban background

Irina Nikolova [a†], A. Rob MacKenzie [a,b], Xiaoming Cai [a], Mohammed S. Alam [a] and Roy M. Harrison [a,c]

---

[a] University of Birmingham, School of Geography, Earth and Environmental Sciences, Edgbaston, B152TT, Birmingham, UK.
[b] Also at Birmingham Institute of Forest Research, Edgbaston, B152TT, Birmingham, UK..
[c] Also at Department of Environmental Sciences / Center of Excellence in Environmental Studies, King Abdulaziz University, PO Box 80203, Jeddah, 21589, Saudi Arabia.
† Corresponding author e-mail: i.nikolova@bham.ac.uk

We developed a model (CiTTy-Street-UFP) of traffic-related particle behaviour in a street canyon and in the nearby downwind urban background that accounts for aerosol dynamics and the variable vapour pressure of component organics. The model simulates the evolution and fate of traffic generated multicomponent ultrafine particles (UFP) composed of a non-volatile core and 17 Semi-Volatile Organic Compounds (SVOC, modelled as n-alkane proxies). A two-stage modelling approach is adopted: (1) a steady state simulation inside the street canyon is achieved, in which there exists a balance between traffic emissions, condensation/evaporation, deposition, coagulation and exchange with the air above roof-level; and (2) a continuing simulation of the above-roof air parcel advected to the nearby urban park during which evaporation is dominant. We evaluate the component evaporation and associated composition changes of multicomponent organic particles in realistic atmospheric conditions and compare our results with observations from London (UK) in a street canyon and an urban park. With plausible input conditions and parameter settings, the model can reproduce, with reasonable fidelity, size distributions in central London in 2007. The modelled nucleation-mode peak diameter, which is 23 nm in the steady-state street canyon, decreases to 9 nm in a travel time of just 120 s. All modelled SVOC in the sub-10 nm particle size range have evaporated leaving behind only non-volatile material, whereas modelled particle composition in the Aitken mode contains SVOC between $C_{26}H_{54}$ and $C_{32}H_{66}$. No data on particle composition are available in the study used for validation, or elsewhere. Measurements addressing in detail the size resolved composition of the traffic emitted UFP in the atmosphere are a high priority for future research. Such data would improve the representation of these particles in dispersion models and provide the data essential for model validation. Enhanced knowledge of the chemical composition of nucleation-mode particles from diesel engine exhaust is needed to predict both their atmospheric behaviour and their implications for human health.

Introduction

Current air quality regulations are set in terms of $PM_{2.5}$ or PM_{10} mass concentrations. However, those mass measurements reflect primarily the accumulation mode and coarse mode particles. Regulatory measures for ultrafine particles (UFP, diameter D_p < 100 nm) have not been introduced, mainly due to insufficient knowledge of the human toxicity of these particles. Recent study suggests that ultrafine particles, by number count, play an important role in the toxicity of airborne particulate matter[1] showing a link between cardiovascular health outcomes with UFP exposure. The majority of UFP in the urban atmosphere arise from road traffic emissions, and road traffic is also recognised to be the largest source of ultrafine particles in the UK national emissions inventory[2]. At a London roadside site, 71.9% of particles by number arise from traffic, with 38% of those in the nucleation mode (D_p < 30 nm) and 53% in the exhaust solid mode (Aitken, 30 < D_p < 100 nm)[3]. Despite large scientific interest, and many contributions to the topic of UFP over the last few decades, the behaviour of ultrafine particles still remains an area with open questions and even contradictory opinions. Specifically open questions remain as to what extent the composition affects the evolution, properties and atmospheric behaviour of UFPs. The chemical composition of particles from engine exhaust is complex, but traffic emitted particles can be approximated as multicomponent organic solutions,associated with coated around refractory graphitic core. Rapid new particle formation and condensation, with a characteristic time-scale of seconds, is responsible for the formation of UFP in the near-wake region of the vehicle. Studies in the wake of vehicles[4-6] show that primary UFP can grow substantially due to condensation of semi-volatile organic compounds (SVOC). Nonetheless, those SVOC are largely uncharacterised because they are unresolved by traditional gas chromatography and often referred to as unresolved complex mixture (UCM). New methods have been developed to investigate which compounds are encapsulated in the UCM, such as two dimensional gas chromatography, a promising method to resolve this complex mixture[7]. Worton and co-authors[8] have reported that traffic induced UFP at a

tailpipe are rich in semi-volatile organic compounds, predominantly n-alkanes, alkyl-cyclohexanes and aromatics. Our own measurements of diesel exhaust composition, analysed with a two dimensional gas chromatography, point as well to the wealth of SVOC[9]. The presence of semi-volatile components within vehicle exhaust particles is responsible for their growth and also has implications for their behaviour in the atmosphere. During the process of dilution downstream from the source, a reduction in vapour and particle concentrations will occur, leading to a shift in favour of evaporation of the SVOC[10].

The evaporation process reduces the UFP diameter, with implications for the efficiency with which they are taken up by inhalation[11]. A study of Dall'Osto and co-authors[12] reports particle size spectra at three sites (street canyon, urban park and tower) in London, UK. They demonstrated a very significant shift in particle size distributions towards smaller sizes during advection from a traffic source to a nearby urban park, at a distance of about 665 metres. The sub-10 nm mode at Regents Park (urban park in London) could potentially arise from localised nucleation processes, but the diurnal pattern and relationship to gaseous pollutants did not show any evidence to support this concept. Particle concentrations correlated with NO_x and black carbon pointing to a traffic source[12]. These findings merit further investigation, by means of numerical simulations, to characterise the evaporative potential and composition changes of the UFP during the advection from the street canyon to the urban park. Typically, in urban areas, high volumes of traffic in street canyons result in some of the highest UFP concentrations due to the limited dilution of the traffic exhaust particles. These hot spots are of great interest due to the possible adverse health effects being attributed to such exposure. Therefore an investigation of the dispersion of UFP and their dynamics within such environments is of growing importance.

A number of studies have reported the modelling of ultrafine particle concentrations in street canyons[13-17], showing great variations in spatial and temporal scales. Other studies have focused on aerosol dynamics (mainly deposition and coagulation), showing the effect of each process on the size distribution[18-20]. A general consensus is that removal processes such as dilution and dry deposition should be considered at street scale[21]. However these studies did not study the volatility of the particles and their complex size-dependent composition given the wealth of traffic-emitted SVOC. There is an apparent gap in the realistic representation of composition of traffic-generated UFP among the street canyon studies. Our aim is to address this gap and develop a model of traffic particle behaviour in a street canyon and in the near vicinity that accounts for the dynamics of the nucleation-mode particles comprised predominantly of organic compounds with a small core of metallic ash or sulphuric acid, with robust insight into the evolution and fate of traffic induced multicomponent UFP in the presence of vapour-phase SVOC. We simulate the evaporation and composition change of multicomponent organic particles in realistic atmospheric conditions and put forward recommendations for further studies.

Methodology

Field measurements: area and meteorology

Data were taken from a measurement campaign which was part of the REPARTEE multi-faceted study of aerosols and gases in the atmosphere of London, UK[22]. Briefly, air sampling was carried out in 2007 between October and November at Marylebone Road and Regents Park, London. The sampling site at Marylebone Road (a street canyon of near unity height/width ratio running approximately WSW-ENE) is on the kerbside of a heavily trafficked London road carrying about 80,000 vehicles per day. Traffic count data were provided from inductive loops in the road. On average the share of Heavy Duty Vehicles was 13.7%. UFP counts and size distributions in the street canyon were determined using Condensation Particle Counters (model TSI 3022A) and a Scanning Mobility Particle Sizer (SMPS, Model 3080 Electrostatic Classifier). The sampling site at Regents Park is about 665 m (Euclidean distance) to the north from the street canyon. It is in the centre of a large area of park, and air sampling from an elevated inlet with a Differential Mobility Particle Sizer consisting of two "Vienna"-style DMAs – an ultrafine DMA for particles of 3.4-34 nm and a standard DMA for particles of 30-830 nm, with TSI model 3025 and 3010 condensation particle counters respectively.

Meteorological data, such as synoptic wind speed and wind direction were obtained from the Heathrow airport site (UK). Days with southerly wind direction, approximately perpendicular to the street canyon axis were selected, in order to evaluate the advection and behaviour of UFP from Marylebone Road to Regent's Park. Mean wind speed for the selected days was 3 m s^{-1}, but the

lowest wind speed was 1.5 m s^{-1}. These wind speeds correspond to minimum travel times from the street canyon to the nearby park of between 222 s and 443 s, respectively. The importance of above-roof-top wind speed and traffic-induced turbulence is addressed in several studies[23-26]. These studies show that for low wind speeds, typically below 1.5 m s^{-1}, the traffic induced turbulence plays a more prominent role in the dilution process. Traffic-induced turbulence was not considered in the present study and its effect on the dilution is neglected. More details on the UFP number counts, size distributions and meteorological conditions can be found elsewhere[12].

Model description

The model system consists of the street canyon model CiTTy-Street[27], which is the urban 'flavour' of the CiTTyCAT trajectory model[28], coupled with a UFP aerosol dynamics module. CiTTy-Street is an urban canopy chemistry model designed to capture the exchange across the street/rooftop concentration gradients in pollutants and in-canyon pollutant deposition of gases, $PM_{2.5}$ and PM_{10}. CiTTy-Street consists of two boxes: the lower box represents either a single canyon or a range of street canyons of height, H, and width, W, within a city. The upper box represents the urban boundary layer, typically with a depth of 1000m. Mixing between the boxes is parameterised using a dimensionless air exchange rate[29] for an above-roof wind perpendicular to the along-canyon axis, which produces in-canyon concentrations matching long-term observations (http://www2.dmu.dk/atmosphericenvironment/Trapos/datadoc.htm;[27]). We have further developed the model to include size-resolved mass and number of UFP. The size range and size resolution considered by the UFP module is user-defined; currently, the UFP module consists of 15 discrete uniform size bins in a logarithmic scale in the size range of 5.8-578 nm. Processes such as dry deposition, coagulation and condensation/evaporation in the presence of SVOC are considered. Dry deposition is based on the resistance scheme described in Seinfeld and Pandis[30] and used in Nikolova and co-authors[20]. The deposition velocity contains a variety of physical processes and is a function of the aerodynamic resistance r_a, the quasi-laminar resistance r_b and the sedimentation speed. Particles deposit on different surfaces like ground, building walls and roofs; the effect of green infrastructure on deposition[28] can be accommodated by varying the deposition resistances. Polydisperse coagulation is also taken into consideration, following the mathematical description in discrete form provided in Seinfeld and Pandis[30] and briefly described in Nikolova and co-authors[20].

The UFP module also accounts for the multicomponent nature of the particles. The driving force for condensation/evaporation is the difference between the partial pressure of each representative SVOC component and its saturation vapour pressure. SVOC measurements of vapour and particulate phases were not conducted during the REPARTEE campaign. However, Harrad and co-authors[31] reported SVOC measurements from Birmingham, which is the second largest city in the UK. Vapour and particulate phases were measured at two sites: Bristol road (BROS), next to a busy traffic road; and at the Birmingham university campus (EROS), an urban background site. The range of SVOC varies from C_{16} to C_{34}, and we have considered SVOC up to C_{32} (Table 1). Harrison and co-authors[32] show that these SVOC are actively partitioning between vapour and particle and are representative of the volatility range of compounds in both ambient airborne and diesel exhaust particles. BROS and EROS SVOC vapour and particulate measurements were used as an initial (in the street canyon) and inlet background (above roof-top) concentrations, respectively. Particles in the model are composed of 17 representative SVOC, however, one more component was added to the system to represent a non-volatile component in the nucleation and Aitken modes in and above the street canyon. The composition of the particles in the nucleation mode is initialised with 1% non-volatile material (by volume), while Aitken-mode particles are mainly non-volatile, having 90% non-volatile material (Table 2), which is discussed in detail in Results and Discussion. These non-volatile particles have grown because of the condensation of semi-volatile material, mainly hydrocarbons, during the dilution stage. Typically, if the pre-existing aerosol concentration is low, homogeneous nucleation is favoured and new particle formation occurs. However, high concentrations of pre-existing particles, promote the condensation of semi-volatile compounds onto these pre-existing particles. Close to the tailpipe, 1-3s after emission, supersaturation may be large enough to trigger nucleation. In addition, in the presence of large surface area of particles, the SVOC and sulphuric acid will condense quickly on the particles, as discussed in Zhang and Wexler[36]. In our study, we have assumed that all processes related to the formation of new particles and subsequent growth and/or condensation onto pre-existing particles have completed before particles reach the kerbside where size distributions are measured. Condensation/evaporation with mass accommodation coefficient $\alpha = 1$,[33] and accounting for the Kelvin effect is treated with a fully-moving-diameter scheme[34] and redistribution onto fixed size

bins in a mass and number conserving approach[35]. Steady-state simulations are performed using the CiTTy-Street-UFP model in and above the street canyon and results for the UFP number size distributions, size resolved composition of the particles and aerosol dynamics are presented in the Results and Discussion. In order to mimic the advection of particles from above roof-top (above Marylebone Road) to the nearby urban park (Regent's Park), we have allowed particles from the upper box (above roof-top) to evolve, using a fully Lagrangian microphysics scheme, for a period equal to the travel time between the two sites. The Lagrangian microphysics scheme allows UFP particles to grow/evaporate to their exact size.

Table 1. Mean vapour and particulate phases of SVOC measured at a busy traffic road (BROS) and urban background (EROS) sites in Birmingham, year 1999/2000. In parenthesis standard deviation (+/-) of the mean. Unit: ng m^{-3}.

	BROS vapour	BROS particulate	EROS vapour	EROS particulate
C16	6.42 (3.62)	0.65 (0.55)	2.47 (1.46)	0.45 (0.41)
C17	9.32 (4.31)	0.85 (0.54)	3.67 (2.36)	0.58 (0.41)
C18	9.36 (4.41)	0.82 (0.43)	3.61 (2.12)	0.47 (0.28)
C19	9.74 (4.09)	1.32 (1.02)	4.07 (1.96)	0.57 (0.38)
C20	8.35 (3.59)	1.93 (1.53)	3.13 (1.41)	0.69 (0.59)
C21	6.20 (3.06)	2.63 (1.84)	2.96 (1.61)	1.31 (1.23)
C22	3.97 (1.98)	3.25 (1.64)	1.64 (0.86)	1.51 (1.54)
C23	2.32 (1.25)	3.73 (1.63)	1.49 (1.35)	2.67 (2.15)
C24	1.59 (1.79)	3.34 (1.70)	0.88 (1.25)	2.51 (2.29)
C25	1.20 (0.52)	4.46 (2.41)	0.78 (0.69)	4.05 (3.42)
C26	1.00 (0.50)	2.37 (1.45)	0.74 (0.43)	3.01 (3.74)
C27	1.28 (0.53)	3.61 (2.46)	0.84 (0.45)	4.49 (4.16)
C28	1.03 (0.53)	1.89 (1.32)	0.76 (0.48)	2.51 (3.42)
C29	1.24 (0.53)	4.89 (3.84)	0.79 (0.46)	5.19 (5.06)
C30	0.80 (0.38)	2.03 (1.26)	0.54 (0.37)	1.94 (2.21)
C31	0.77 (0.30)	3.60 (3.23)	0.50 (0.32)	3.81 (4.78)
C32	0.42 (0.18)	1.32 (0.89)	0.28 (0.21)	1.07 (1.31)

Table 2. Particles composition for nucleation mode (NM) and Aitken mode (AiM) for all input organic components expressed as % of the volume concentration. Above roof top composition is used for initial and inlet background concentrations.

	Particulate mass fractions NM		Particulate mass fractions AiM	
Component	street canyon	above roof top	street canyon	above roof top
Non-volatile	1.0	1.0	90.0	90.0
C16	1.5	1.2	0.3	0.3
C17	2.0	1.6	0.8	1.0
C18	1.9	1.3	0.5	0.5
C19	3.1	1.5	1.1	1.4
C20	4.5	1.8	0.4	0.7
C21	6.1	3.5	0.8	1.2
C22	7.5	4.1	0.6	0.8
C23	8.7	7.2	1.0	1.1
C24	7.8	6.7	0.8	0.7
C25	10.4	10.9	0.9	0.7
C26	5.5	8.1	0.8	0.4
C27	8.4	12.1	0.6	0.4
C28	4.4	6.7	0.5	0.2
C29	11.4	13.9	0.3	0.2
C30	4.7	5.2	0.2	0.1
C31	8.3	10.3	0.2	0.2
C32	3.1	2.9	0.2	0.1

Results and Discussion

Stage 1: Modelling in-canyon processes

The steady state model output is analysed in the street canyon (Marylebone Road) and the size distribution is plotted in Figure 1. In addition on the same figure we present the 'inlet' background size distribution (i.e., the background size distribution that is advected into the above-roof box by the mean wind) and the size-resolved emission distribution, in order to illustrate the relative influences on the steady state size distribution from the background and the emissions, respectively. The size resolved emissions are initialised with a bi-modal log normal distribution, with geometric mean diameters in nucleation and Aitken modes at 35 nm and 65 nm, respectively (Figure 1). The modelled size distribution peaks in the nucleation mode with a geometric mean diameter at 23 nm and is followed by a small shoulder in the Aitken mode. The nucleation mode, which is semi-volatile, makes an important contribution to total particle number close to traffic sources[3]. The total number of particles in the street canyon at steady state for a wind speed of 1.5 m s^{-1} is 54500 # cm^{-3}.
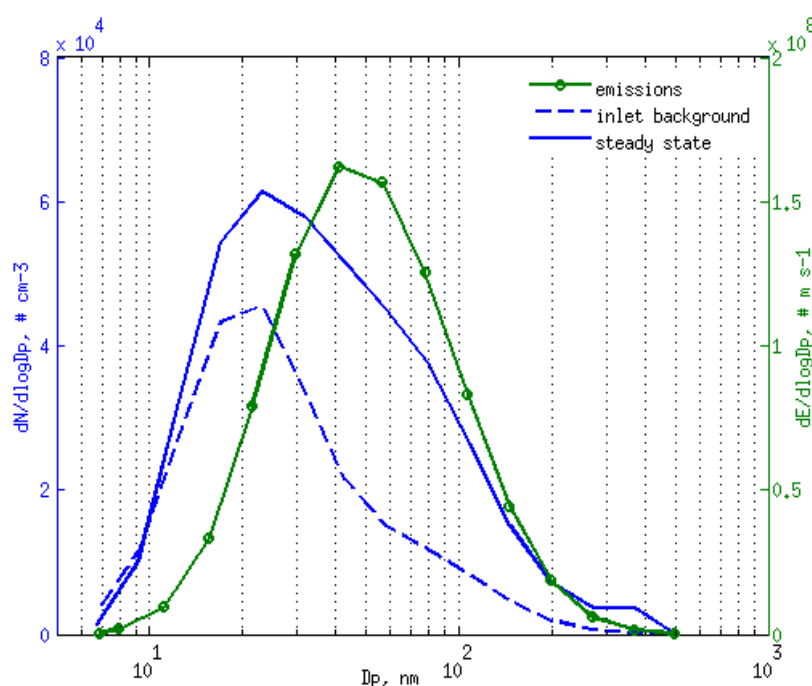

Figure 1. Steady state number size distribution in the street canyon (Marylebone Road) for a cross-canyon wind speed of 1.5 m s^{-1}. On the same figure, the inlet background size distribution and the size resolved emission distribution are plotted to illustrate the relative influences on the steady state size distribution from the background and the emissions, respectively.

Role of deposition and coagulation in the street canyon

Deposition and coagulation are the processes that reduce the number of particles per size bin and therefore the total number of particles. Their overall effect depends on factors such as particle number concentration, particle diameter, state of the atmosphere, wind speed, the nature of the deposition surface, etc. For PM$_{2.5}$ and chemical tracers, Pugh and co-authors[27] describe the relative importance of in-canyon deposition as a function of canyon retention-time, defined and discussed below. We have examined the effect of deposition and coagulation on the steady state particle size distribution inside the street canyon (cf. Figure 1) for a wind speed of 1.5 m s^{-1} and 3.0 m s^{-1}, respectively. The steady state total number concentration without any deposition and coagulation is 59400 # cm^{-3} and 35200 # cm^{-3}, respectively. Deposition reduces the total number concentration by 4.1% (for wind speed 1.5 m s^{-1}) and by 3.4 % (for wind speed 3 m s^{-1}), see Table 3. The rate of coagulation is found to be faster than that of deposition for a wind speed of 1.5 m s^{-1}, with an overall 4.8% reduction in the total number concentration at steady-state. However, the role of coagulation in the well-mixed street canyon is diminished with an increase in the wind speed. Particle concentration decreases only by 1.7% for a wind speed of 3 m s^{-1}. The overall

reduction of particle numbers due to the combined effect of deposition and coagulation is 8.2% for 1.5 m s^{-1} and 4.7% for 3 m s^{-1} wind speeds. Deposition is found to be faster than coagulation for the steady state size distribution inside the street canyon for wind speeds above 2 m s^{-1} (Table 3).

Table 3. Reduction in total number of particles in the street canyon (%) for different wind speeds and accounting for different processes. All comparisons are against a base case steady-state solution without coagulation or deposition.

Wind speed, m s^{-1}	Coagulation +deposition	Coagulation	Deposition	Total number UFP, # cm^{-3}
1.5	8.2	4.8	4.1	59400
2	6	2.7	3.5	47200
3	4.7	1.7	3.4	35200

In terms of reduction of particles concentration per size bin, losses due to deposition at low wind speed (1.5 m s^{-1}) for particles with diameter of 6.7nm can reach up to 19%, while losses due to coagulation are higher, approximately 25%. With the increase of particle diameter, losses per size bin decrease as shown in Figure 2. In the case of wind speed of 3 m s^{-1}, deposition losses in the smallest size bin (6.7 nm) are approximately 20%, while the loss due to coagulation is about 15% (Figure 3). Deposition remains faster in reducing the number of particles per size bin than coagulation for particles with diameter below 50 nm.
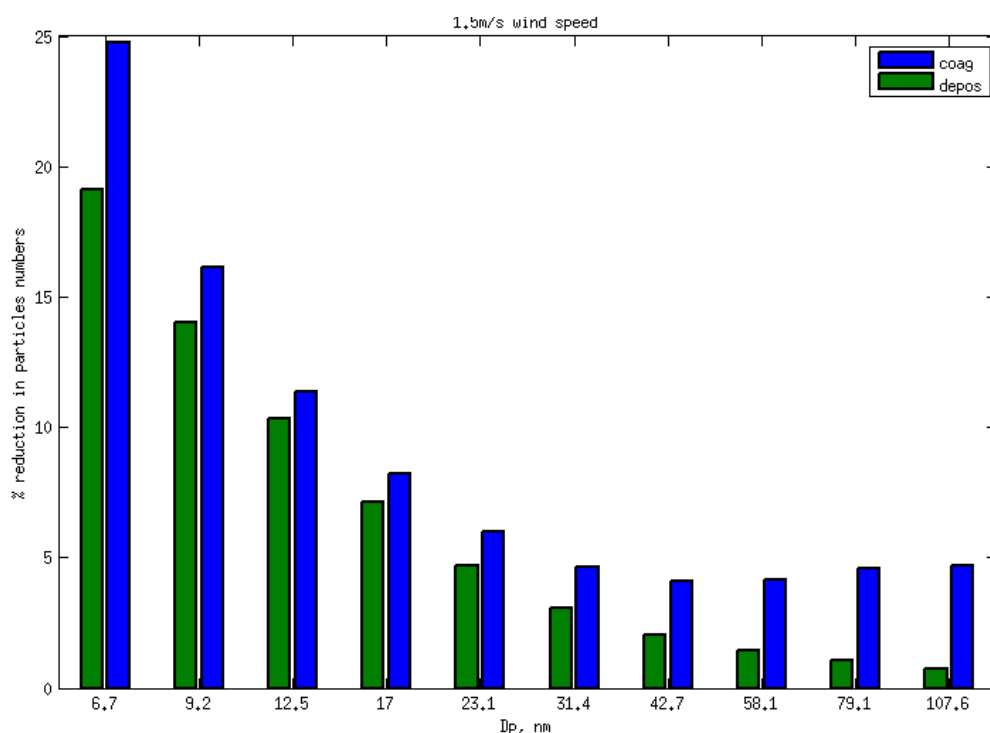

Figure 2. Reduction in particles number concentration in the street canyon (%) due to coagulation and deposition per size bin at wind speed of 1.5 m s^{-1}.
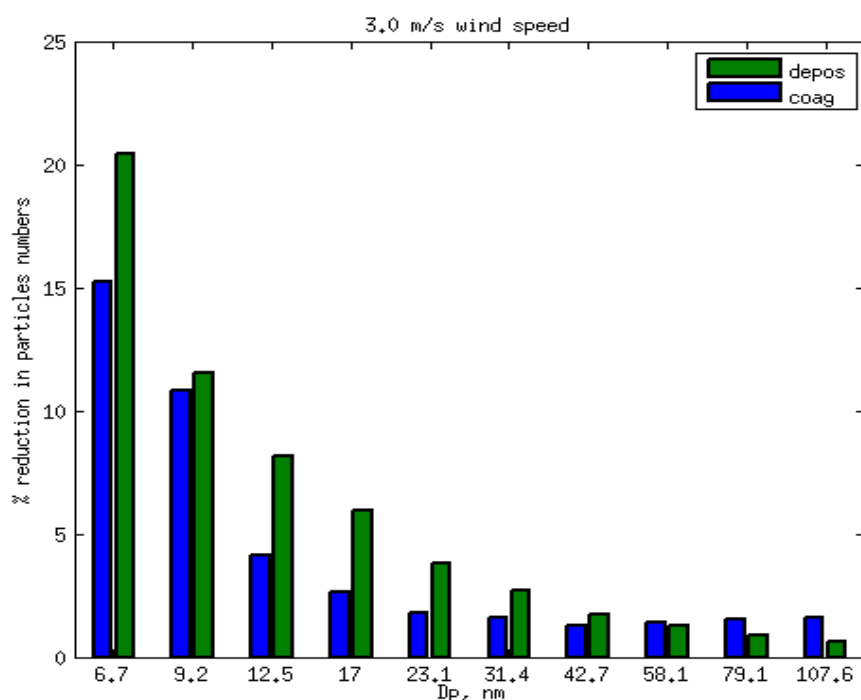
Figure 3. Reduction in particles number concentration in the street canyon (%) due to coagulation and deposition per size bin at wind speed of 3 m s⁻¹.

There are different opinions on the importance of deposition and coagulation in the literature. For example Gidhagen and co-authors[13] found that losses at kerbside due to deposition and coagulation are overall small and typically less than 10% with deposition being faster for higher wind speeds than coagulation. Deposition and coagulation were most effective for the smallest ultrafine particles, which is in line with our findings. Nikolova and co-authors[16] show that during the 'road-to-ambient' dilution stage, dilution is the major mechanisms in altering the aerosol size distribution, while coagulation and deposition play minor roles. Kumar and co-authors[37] also supports the view that coagulation at street scale could be neglected especially when particles with diameter less than 10 nm are not considered. Based on the urban scale modelling study of Ketzel and Berkowicz[21], deposition plays a more pronounced role in reducing the total particle number concentration than coagulation. Several studies[20, 38-40] agree on the negligible role of coagulation in the street environment. However, Li and co-authors[41] have measured particle size distributions at different heights in a street canyon and have argued that the shift in the peak diameter in the Aitken mode to larger diameters is attributed to the effect of coagulation. Stagnant air flows favour the increased particle number concentration through reduced vertical dispersion that may promote particle to particle coagulation. The role of deposition in Li and co-authors[41] in reducing particle number concentrations was not addressed and the measured decrease in particle number concentration with height was mainly attributed to dilution and coagulation.Zhu and co-authors[42] reported that atmospheric dilution and coagulation played substantial roles in the rapid decrease of the ultrafine particle concentration and transformation of the size distribution; however, their study was near to a highway. Overall, the removal of particles due to deposition and coagulation depends on a number of factors such as particle number concentration, particle diameter, ventilation in and out of a street canyon, the complexity of the urban area which influences the air flow between buildings, etc.[43,44] and so cannot, in general, be neglected. Nonetheless, all studies agree that the prime mechanism of reducing particle number concentration is dilution. Time-scale analysis elucidates the relative importance of the removal processes, as suggested in Ketzel and Berkowicz[19]. We have evaluated the characteristic timescales for dilution, deposition, and coagulation. Dilution is the fastest process with a time scale of 147 s for a wind speed of 1.5 m s⁻¹ and canyon height of 22 m, followed by coagulation (250 s), and then deposition (288 s). Dilution remains the fastest process in reducing the particle number concentration for a wind speed of 3 m s⁻¹ with a time scale of 73 s, while deposition and coagulation have much slower time scales of 320 s and 500 s, respectively. That is, as above-roof

wind speed increases, the scale separation between dilution and the microphysical processes also increases, leading to an increasing dominance of dilution over other processes in determining the steady-state. Another useful parameter in the diagnosis of the model dynamic system is the so-called retention time $\tau = H/w_e$, where H is the building height and w_e is the exchange velocity, which is linearly proportional to the background reference wind speed above the roof level. Cai[45] shows that the exchange coefficient (i.e., the constant of proportionality between w_e and the above-roof mean wind), based on large eddy simulation (LES) for a unity canyon aspect ratio, is about 0.01 for a neutrally stratified atmosphere. For H = 22 m and wind speed at roof-top of 1.5 m s^{-1}, τ is approximately 1467 s. For wind speed at roof-top of 3 m s^{-1}, τ is about 733 s. In both cases we see the large retention time in the street canyon and, hence, the opportunity for the ultrafine particles to reach a steady state as well as for in-canyon microphysics to influence the size distribution within and above the canyon. Pugh and co-authors[27] (see especially their Figure 3) find that in-canyon steady-state $PM_{2.5}$ mass concentrations are a strong function of deposition velocity for $\tau > 100$ s. Given the strong dependence of deposition efficiency on particle size in the ultra-fine size range (Figures 2 and 3), we can deduce that increasing the deposition surface without increasing τ, e.g. by judicious use of green infrastructure, will greatly reduce nucleation-mode number concentrations.

Stage 2: Above roof-top and downwind advection: the role of SVOC on particle behaviour
Above roof-top, the steady-state size distribution is plotted in Figure 4 along with the inlet background size distribution. The modelled total number of particles above roof-top is ~30,500 # cm^{-3}, i.e., 56% of the in-canyon steady-state concentration. Particles from above roof-top are subject to
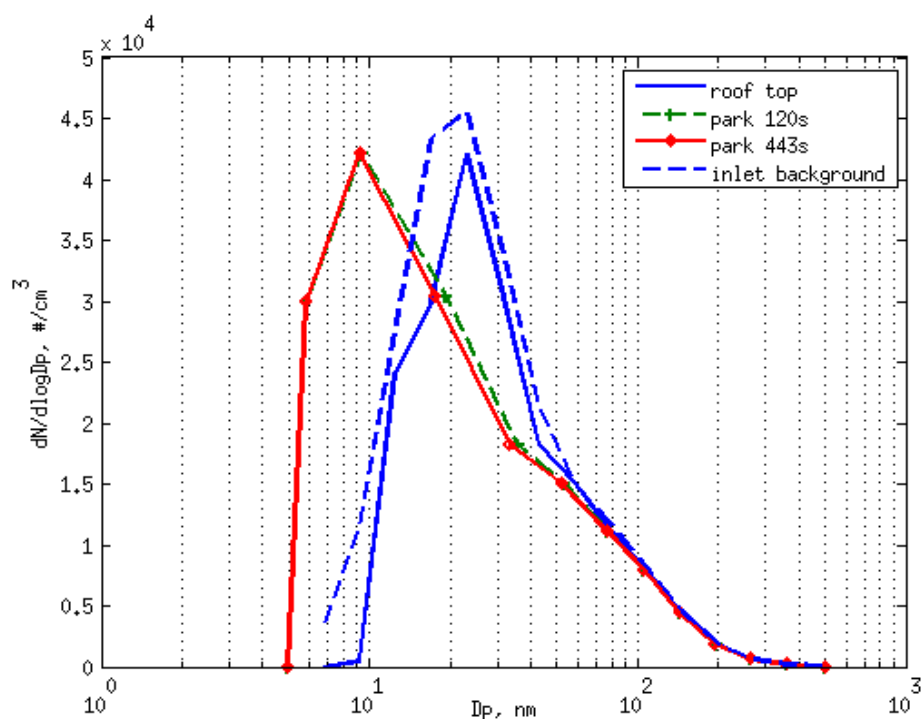

Figure 4. Particle size distributions due to the mixing of particles between the street canyon air and above roof-top (labelled 'roof-top'), the inlet background size distribution ('inlet background') and during advection from above roof-top to the urban park plotted at two selected times.

condensation/evaporation for a time similar to that for advection between the street canyon (Marylebone Road) and urban park using a fully Lagrangian size-distribution solver. For the lowest wind speed of 1.5 m s^{-1} and distance between the two sites of 665 m, the travel time is at least 443 s. The distribution after 443 s is plotted in Figure 4. A remarkable shift in the nucleation-mode particles is modelled, with very little effect on particle diameter in the Aitken mode. The modelled 23 nm geometric mean diameter in the nucleation mode has shrunk to ~9 nm, consistent with the

measurements in the urban park, which showed a peak at D_p ~7-8 nm[12]. Moreover, the remarkable shift in particle diameter in the nucleation mode happens in ~120s, which is much faster than the travel time between the street canyon and the park. Vertical mixing in the urban boundary layer is neglected due to the relatively large time scale involved, which is ca. 10 min in conditions of high turbulence and more than 20 min in stable condition[47]. For a wind speed of 3 m s^{-1} at roof-top, the travel time to the urban park would be ~222 s, nearly twice as large as the modelled time of ~120 s for the detection of a major diameter shift. In the sub-10nm-diameter particle size range, the n-alkanes in the range $C_{16}H_{34}$-$C_{22}H_{46}$ have entirely evaporated and the particles are solely composed of the non-volatile material (see Table 4). Particles with initial D_p = 31 nm have shrunk to D_p = 18 nm and are composed of a non-volatile material and the slowly evaporating $C_{31}H_{64}$ and $C_{32}H_{66}$. Aitken-mode particles continue to contain $C_{26}H_{54}$-$C_{32}H_{66}$ SVOCs, although in relatively low concentrations compared to the concentration of non-volatile material. N-alkanes in the range $C_{24}H_{50}$-$C_{32}H_{66}$ can be found in all particles in the accumulation mode (D_p > 100 nm), while $C_{23}H_{48}$ is present in particles with $D_p \geq 143$ nm at the end of the simulation.

Table 4. Component mass-size distributions, dM/dlogDp (ng m^{-3}), after advection from the street canyon to the urban park. Dp is particle diameter (in nm) after evaporation to exact size. 'Dp < 5nm' indicates that the distribution goes beyond the lower bin bound and therefore concentration for all components is set to 0. Initial Dp (in nm): particle diameter at roof-top at steady state. SVOC concentration for particles with Dp > 5nm are set to 0 in the table when the concentration for that component is less than 0.005 ng m^{-3}. dlogDp = 0.1337.

Non-volatile mass, μg/m³	C32	C31	C30	C29	C28	C27	C26	C25	C24	C23	C22	C21	C20	C19	C18	C17	C16	Total mass μg/m³	Dp nm	Initial Dp nm
0	0.00	0.00	0.00	0.00	0.00	0.00	0.00	0.00	0.00	0.00	0.00	0.00	0.00	0.00	0.00	0.00	0.00	0	<5	7
0	0.00	0.00	0.00	0.00	0.00	0.00	0.00	0.00	0.00	0.00	0.00	0.00	0.00	0.00	0.00	0.00	0.00	0	<5	9
0	0.00	0.00	0.00	0.00	0.00	0.00	0.00	0.00	0.00	0.00	0.00	0.00	0.00	0.00	0.00	0.00	0.00	0	<5	12
0.00309	0.00	0.00	0.00	0.00	0.00	0.00	0.00	0.00	0.00	0.00	0.00	0.00	0.00	0.00	0.00	0.00	0.00	0.00309	6	17
0.0173	0.00	0.00	0.00	0.00	0.00	0.00	0.00	0.00	0.00	0.00	0.00	0.00	0.00	0.00	0.00	0.00	0.00	0.0173	9	23
0.0847	0.42	0.14	0.00	0.00	0.00	0.00	0.00	0.00	0.00	0.00	0.00	0.00	0.00	0.00	0.00	0.00	0.00	0.0852	18	31
0.3407	4.51	6.46	0.91	0.27	0.00	0.30	0.00	0.00	0.00	0.00	0.00	0.00	0.00	0.00	0.00	0.00	0.00	0.3531	33	43
1.074	6.34	12.73	3.36	2.30	0.35	2.34	0.00	0.00	0.00	0.00	0.00	0.00	0.00	0.00	0.00	0.00	0.00	1.101	52	58
2.597	6.10	11.92	4.84	4.95	1.31	5.60	0.16	0.00	0.00	0.00	0.00	0.00	0.00	0.00	0.00	0.00	0.00	2.632	77	79
4.783	6.79	10.04	5.80	5.91	2.87	9.02	0.33	0.18	0.11	0.00	0.00	0.00	0.00	0.00	0.00	0.00	0.00	4.824	105	108
6.700	8.56	11.03	7.69	7.68	5.54	14.64	0.87	0.27	0.16	0.13	0.00	0.00	0.00	0.00	0.00	0.00	0.00	6.757	143	146
7.136	9.15	11.70	8.75	9.21	8.14	18.99	2.80	0.71	0.19	0.14	0.00	0.00	0.00	0.00	0.00	0.00	0.00	7.206	195	199
5.780	7.52	9.75	7.55	8.41	8.36	17.83	5.77	2.72	0.38	0.12	0.00	0.00	0.00	0.00	0.00	0.00	0.00	5.848	265	271
3.563	4.68	6.14	4.85	5.63	6.01	12.09	6.61	5.30	1.33	0.13	0.00	0.00	0.00	0.00	0.00	0.00	0.00	3.616	360	369

Discussion

The entrained lubricating oil from cylinder walls is partially burned and together with unburned fuel is responsible for the organic carbon associated with the diesel exhaust particles. The formation of nucleation-mode particles is driven by the concentration of the nucleating species, mainly sulphuric acid and hydrocarbons. During dilution and cooling of the exhaust plume, volatile precursors may become sufficiently supersaturated to nucleate new particles and promote growth of existing particles. These vapour precursors may also be subject to gas-to-particle conversion by adsorption onto the accumulation mode, thus reducing the concentration of precursors and, hence, the driving force for nucleation and subsequent growth. Therefore, for a given concentration of precursors, nucleation and growth will be suppressed by existing accumulation-mode particles. Current legislation standards aim at reducing the mass concentration of the accumulation-mode particles, hence unintentionally promote the formation of nucleation-mode particles. The studies of Sakurai and co-authors[47], Tobias and co-authors[48], Ziemann and co-authors[49] suggest that the nucleation-mode particles consists primarily of heavy hydrocarbons mainly associated with lubrication oil. However, there is still debate regarding the existence of non-volatile material in particles in the nucleation mode, while studies broadly agree on the predominance of non-volatile material in the Aitken mode. Biswas and co-authors[50] point out that the smallest particles (~20 nm) in the vicinity of a highway are predominantly volatile, shrinking

below the lower cut-off size of their SMPS (~7 nm), while the remaining particles in the upper nucleation mode shrink down to ~10 nm. Aitken-mode particles (D_p > 40 nm) show evidence of external mixing with a non-volatile fraction that increases with particle diameter. The 80 nm particles, which are a good indicator of soot aerosol emissions, had the highest non-volatile fraction of all particle sizes[50]. Similar findings are reported in Tiitta and co-authors[51] from a thermodenuder study of roadside ultrafine particles. They show a major fraction of nucleation-mode particles that have partly evaporated with a non-volatile core of 10 nm whereas the non-volatile constituents are dominant in the Aitken-mode particles. [4] found that more than 97% of the volume of 12 and 30 nm particles evaporated when heated to 400ºC, which is consistent with the volatility of $C_{24}H_{50}$-$C_{32}H_{66}$. Such heavy alkanes are more prevalent in lubricating oil than in fuel[49, 52]. According to Ronkko and co-authors[53], particle size distributions measured after a thermodenuder consist of two modes with geometric mean diameters smaller than 9 nm and 37-47 nm, indicating that both the nucleation-mode and Aitken-mode particles contain non-volatile material. The non-volatile material (core) of the particles is formed under high temperature conditions, most likely in the combustion chamber. Nonetheless, the formation mechanism and the composition of these non-volatile fractions are unresolved due to the limited experimental data and sampling challenges. Ronkko and co-authors[54] discuss the existence of a non-volatile fraction in the nucleation-mode particles with or without after-treatment equipment and point out that the non-volatile diameter is typically below 7 nm. Kirchner and co-authors[55] show that during cold start and idle not all nucleation-mode particles are removed after being heated in the thermodenuder at 280ºC. Particles with a diameter of 30-40 nm shrunk to 10-20 nm having smaller spots (1-3 nm) with very high contrast when examined under TEM (transmission electron microscopy). Birmili and co-authors[56] express the view that all particles above 12 nm contain a non-volatile material. On the other hand, Wehner and co-authors[57] did not detect any non-volatile material in their thermodenuder measurements of traffic influenced particles near a highway. They found that the nucleation-mode particles appear to be completely volatile, while 30 nm particles have non-volatile material above the instrument cut-off size of 10 nm. Nearly all the particles in the upper Aitken (~80 nm) and lower accumulation mode (~150 nm) contain a non-volatile core with a thickness of the volatile layer below 10% of particle radius.

Our approach of considering a non-volatile fraction in both the nucleation and Aitken modes is in line with the studies discussed above. We show that under meteorological conditions at the time, in order to explain the evaporative diameter shrinkage in the nucleation-mode particles measured by Dall'Osto and co-authors[12] in London particles in the nucleation mode should have 99% by volume of volatile material in the 23 nm particles. In addition, we have performed sensitivity analysis to assess the importance of the non-volatile fractions on the size distribution and the overall role of evaporation. By increasing the non-volatile material from 1% to 3% in the nucleation mode in both model stages, we simulate a diameter shrinkage from 23 nm to 11.6 nm, i.e ~97% of the 23 nm particle's volume is volatile. Measurements of the UFP composition in the street canyon and the urban park are not currently available, which hinders our model validation for the UFP composition at this stage. Moreover, the health effects of particles containing non-volatile material are still unknown[54]. The non-volatile material contains mainly carbon and possibly some metal oxides from the engine lubricant and sulphate from oxidation of S in the fuel. Li and co-authors[58] show that an emitting diesel truck during idle induce a high level of oxidative stress in human aortic endothelial cells, mainly related to the type of metals and trace elements. However, the emissions from the same diesel truck under urban dynamometer driving cycle induce pro-inflammatory response, attributed to the enriched content of organic species. Xia and co-authors[59] show that traffic-related UFP, enriched in polycyclic and other semivolatile hudrocarbons, act to promote allergic airway inflammation. The relative importance of these particles in creating a health risk from exposure warrant further investigations.

Conclusions

We have developed a model (CiTTy-Street-UFP) of traffic-emitted particle behaviour in a street canyon and in the near vicinity that accounts for particle dynamics, the complex mixing between particles with different compositions and considers the multicomponent nature of the UFP in the presence of 17 SVOC (modelled as n-alkane proxies). We evaluated the UFP evaporative potential and composition changes of multicomponent organic particle under realistic atmospheric conditions. Steady state simulations were performed in a street canyon and above roof-top. The above-roof-top UFP size distribution was advected to the nearby urban park during which particles were allowed to grow/shrink to their exact size. We found that during the advection, particles in

the nucleation mode shrunk remarkably in agreement with the measurements of Dall'Osto and co-authors[12]. The modelled nucleation-mode peak diameter at 23 nm decreased to 9 nm in 120 s, much less than the straight-line travel time between sites even at roof-top wind speeds of 3 m s^{-1}. No SVOC remained in the sub-10 nm range, only non-volatile material remained. In order to simulate the nucleation-mode UFP observed, therefore, we require either involatile cores in the nucleation-mode particles emitted from the street canyon, or a composition consisting in part of organic compounds with volatilities much lower than those of $C_{32}H_{66}$ n-alkanes. Particles in the Aitken mode had SVOC present between $C_{26}H_{54}$ and $C_{32}H_{66}$. Although we found a very good agreement between model and measured results for the overall shape of the size distribution, there is no data on particle composition in the urban park with which to validate the composition aspect of our results. Moreover, robust UFP composition measurements at street scale are lacking. Measurements devoted to address in detail the composition of the traffic emitted UFP in the atmosphere are required. This would improve the representation of these particles in dispersion models and provide data for model validation. In addition, the robust representation of the chemical composition would provide more insights into the mechanisms of mixing in the atmosphere, the typical lifetime and overall behaviour of the traffic-emitted ultrafine particles. Data on UFP composition will allow an assessment of the complex spatial and temporal composition variations at or close to traffic sites. Such data would provide information on possible trends and help identify the non-volatile and the volatile materials of relevance for future epidemiological and toxicological studies investigating health effects of UFP.

Acknowledgements

References

1 R. W. Atkinson, G. Fuller, R. Anderson and P. M. Harrison, *Epidemiology*, 2010, 21, 4, 501-511.
2 AQEG, Air Quality Expert Group, Department for Environment, Food and Rural Affairs Defra, London, 2005.
3 R. M. Harrison, D. C. S. Beddows and M. Dall'Osto, *Environ. Sci. Technol.*, 2011, 45, 5522–5528.
4 D. B. Kittelson, W. F. Watts and Johnson, J. P., *J. Aerosol Sci.*, 2006, 37, 913-930.
5 U. Uhrner, S. Von Lowis, H. Vehkamaki, Wehner, B. Brasel, M. Hermann, F. Stratmann, M. Kulmala, M. and A. Wiedensohler, *Atmos. Environ.*, 2007, 41, 7440-7461.
6 B. Albriet, K. N. Sartelet, S. Lacour, B. Carissimo and C. Seigneur, *Atmos. Environ.*, 2010, 44, 1126-1137.
7 A. W. H. Chan, G. Isaacman, K. R. Wilson, D. R. Worton, C. R. Ruehl, T. Nah, D. R. Gentner, T. R. Dallmann, T. W. Kirchstetter, R. A. Harley, J. B. Gilman, W. C. Kuster, J. A. de Gouw, J. H. Offenberg, T. E. Kleindienst, Y. H. Lin,C. L. Rubitschun, J. D. Surrat, P. L. Hayes, J. L. Jimenez and A. H. Goldstein, *J. Geophys. Res.*, 2013, 118, 6783-6796.
8 D. R. Worton, G. Isaacman, D. R. Gentner, T. R. Dallmann, A. W. H. Chan, C. Ruehl, W. Kirchstetter, K. R. Wilson, R. A. Harley and A. H. Goldstein, *Environ. Sci. Technol.*, 2014, 48 (7), 3698-3706.
9 M. S. Alam, S. Z. Rezaei, C. P. Stark, Z. Liang, H. M. Xu and R. M. Harrison. Faraday Discussion, Chemistry of Urban Atmosphere, 2016
10 A. L. Robinson, N. M. Donahue, M. K. Shrivastava, E. A. Weitkamp, A. M. Sage, A. P. Grieshop, T. E. Lane, J. R. Pierce and S. Pandis, *Science*. 2007, 315, 1259-1262.
11 R. M. Harrison, R.M.,C. Giorio, D. C. Beddows and M. Dall'Osto, *Sci. Total Environ.*, 2010, 409, 289-293.
12 M. Dall'Osto, A. Thorpe, D. C. S. Beddows, R. M. Harrison, J. F. Barlow, T. Dunbar, P. I. Williams and H. Coe, *Atmos. Chem. Phys.*, 2011, 11, 6623-6637.
13 L. Gidhagen, C. Johansson, J. Langner and V. Foltescu, *Atmos. Environ.*, 2005, 39, 1711–1725.
14 A. Abdulsaheb and P. Kumar., *18th International Symposium on Transport and Air Pollution*, 2010, 1–6.
15 P. Kumar, A. Garmory, M. Ketzel, R. Berkowicz and R. Britter, *Atmos. Environ.*, 2009, 43, 949-958.
16 I. Nikolova, S. Janssen, K. Vrancken, P. Vos, V. Mishra and P. Berghmans, *Sci. Total Environ.*, 2011, 412, 336-343.
17 G. Habilomatis and A. Chaloulakou, *Sci. Total Environ.*, 2015, 530–531, 227-232.
18 L. Gidhagen, C. Johansson, J. Langner and G. Olivares, *Atmos. Environ.*, 2004, 38, 2029–2044.
19 M. Ketzel and R. Berkowicz, *Atmos. Environ.*, 2004, 38, 2639-2652.
20 I. Nikolova, S. Janssen, P. Vos and P. Berghmans, *Aerosol Air Qual. Res.*, 2014, 14, 145-155.
21 M. Ketzel and R. Berkowicz, *Atmos. Environ.*, 2005, 39, 3407-3420.
22 R. M. Harrison, M. Dall'Osto, M., D. C. S. Beddows, A. J. Thorpe, J. Allan, H. Coe, J. Dorsey, M. Gallagher, C. Martin, J. Whitehead, P. Williams, A. K. Benton, R. L. Jones, J. Langridge, S. Ball, B. Langford, C. N. Hewitt, B. Davison, D. Martin, K. Petersson, S. J. Henshaw, I. R. White, D. E. Shallcross, J. F. Barlow, T. Dunbar, F. Davies, E. G. Nemitz, G. Phillips and C. Helfter, *Atmos. Chem. Phys.*, 2012, 12, 3065-3114.
23 N. A. Mazzeo and L. E. Venegas, *Int. J. Environ. Pollut.,* 2005, 25, 1-4.

24 S. Di Sabatino, P. Kastner-Klein, R. Berkowicz, R. E. Britter and E. Fedorovich, *Environ. Fluid Mech.*, 2003, 3 (2), 129-143.

25 P. Kastner-Klein, E. Fedorovich, M. Ketzel, R. Berkowicz and R. Britter, *Environ. Fluid Mech.*, 2003, 3, 145–172.

26 E. Solazzo, S. Vardoulakis and X. Cai, X., *Atmos. Environ.*, 2007, 41, 5357–5370.

27 T. A. M. Pugh, A. R. MacKenzie, et al., *Environ. Sci. Technol.*, 2012a, 46, 7692–7699.

28 T. A. M. Pugh, M. Cain, J. Methven, O. Wild, S. R. Arnold, E. Real, K. S. Law, K. M. Emmerson, S. M. Owen, J. A. Pyle, C. N. Hewitt and A. R. MacKenzie, *Geosci. Model Dev.*, 2012b, 5, 193-221.

29 C. -H. Liu, D. Y. C. Leung, and M. C. Barth, *Atmos. Environ.*, 2005, 39, 1567-1574.

30 J. H. Seindfeld and S. N. Pandis, Atmospheric Chemistry and Physics, 1998, Wiley, New York.

31 S. Harrad, S. Hassoun, M. S. C. Romero, R. M. Harrison, *Atmos. Environ.*, 2003, 37, 4985-4991.

32 R. M. Harrison, A. M. Jones, D. C. Beddows, M. Dall'Osto and I. Nikolova, *Atmos. Environ.*, 2016, 125, 1-7.

33 J. Julin, P. M. Winkler, N. M. Donahue and P. E. Wagner, *Environ. Sci. Technol.*, 2014, 48, 12083-12089.

34 M. Z. Jacobson, *Aerosol Sci. Technol.*, 1997, 27, 491-498.

35 E. Debry, K. Fahey, K. Sartelet, B. Sportisse and M. Tombette, *Atmos. Chem. Phys.*, 2007, 7, 1537–1547.

36 K. M. Zhang and A. S. Wexler, *Atmos. Environ.*, 2004, 38 (38), 6643–6653.

37 P. Kumar, M. Ketzel, S. Vardoulakis, L. Pirjola and R. Britter, *J Aerosol Sci.*, 2011, 42, 580–603.

38 E. Vignati, R. Berkowicz, F. Palmgren, E. Lyck and P. Hummelshoj, *Sci. Total Environ.*, 1999, 235, 37-49.

39 M. Pohjola, L. Pirjola, J. Kukkonen and M. Kulmala, *Atmos. Environ.*, 2003, 37, 339–351.

40 L. Pirjolaa, T. Lähdea, J. V. Niemic, A. Kousac, T. Rönkköe, P. Karjalainene, J. Keskinene, A. Freyf and A. Hillamof, *Atmos. Environ.*, 2012, 63, 156–167.

41 X. L. Li, J. S. Wang, X. D. Tu, W. Liu and Z. Huang, *Sci. Total Environ*, 2007, 378, 306-316.

42 Y. Zhu, W. Hinds, S. Kim, S. Shen and C. Sioutas, *Atmos. Environ.*, 2002, 36. 4323-4335.

43 B. Wehner, W. Birmili, T. Gnauk and A. Wiedensohler, *Atmos. Environ.*, 2002, 36, 2215-2223.

44 A. Charron and R. M. Harrison,R.M., *Atmos. Environ.*, 2003, 37, 4109-4119.

45 X. Cai, *Atmos. Environ.*, 2012, 51, 268-277.

46 J. F. Barlow, T. M. Dunbar, E. G. Nemitz, C. R. Wood, M. W. Gallagher, F. Davies, E. O'Connor and R. M. Harrison, *Atmos. Chem. Phys.*, 2011, 11, 2111-2125.

47 H. Sakurai, P. Park, P. H. McMurry, D. D. Zarling, D. B. Kittelson and P. J. Ziemann, *Environ. Sci. Technol.*, 2003b, 37, 5487–5495.

48 H. Tobias, D. E. Beving and P. J. Ziemann, *Environ. Sci. Technol.*, 2001, 35 (11), 2233-2243.

49 P. Ziemann, H. Sakurai and P. H. McMurry, Final report, CRC Project no. E-43-4, 2002.

50 S. Biswas, L. Ntziachristos, K. Moore and C. Sioutas, *Atmos. Environ.*, 2007, 41 (16), 3479-3493.

51 P. Tiitta, P. Miettinen, P. Vaattovaara, J. Joutsensaari, T. Petaja, A. Virtanen, T. Raatikainen, P. Aalto, H. Portin, S. Romakkaniemi, H., Kokkola, K. E. J. Lehtinen, M. Kulmala and A. Laaksonen, *Atmos. Environ.*, 2010, 44 (7), 976-986.

52 H. Sakurai, H. J. Tobais, K. Park, D. Zarling, K. S. Docherty, D. B. Kittelson, P. H. McMurry and P. J. Ziemann, *Atmos. Environ.*, 2003a, 37, 1199–1210.

53 T. Ronkko, A. Virtanen, J. Kannosto, J. Keskinen, M. Lappi and L. Pirjola, E*nviron. Sci. Technol.*, 2007, 41, 6384-6389.

54 T. Ronkko, T. Lahde, J. Heikkila, L. Pirjola, U. Bauschke, F. Arnold, H. Schlager, D. Rothe, J. Yli-Ojanpera and J. Keskinen, *Environ. Sci. Technol.*, 2013, 47, 11882-11889.

55 U. Kirchner, V. Scheer, R. Vogt and R. Kägi, *J. Aerosol Sci.*, 2009, 40 (1), 55-64.

56 W. Birmili, K. Heinke, M. Pitz, J. Matschullat, A. Wiedensohler, J. Cyrys, H. -E. Wichmann and A. Peters, *Atmos. Chem. Phys.*, 2010, 10, 4643–4660.

57 B. Wehner, S. Philippin, A. Wiedensohler, V. Scheer and R. Vogt, *Atmos. Environ.*, 2004, 38 (36), 6081-6090.

58 R. Li, Z. Ning, R. Majumdar, J. Cui, W. Takabe, N. Jen, C. Sioutas and T. Hsiai. Part. Fibre Toxicol., 2010, 7-6.

59 M. Xia, L. Viera-Hutchins, M. Garcia-Lloret, M. N. Rivas, P. Wise, S. A. McGhee, Z. K. Chatila, N. Daher, C. Sioutas and T. A. Chatila. *J. Allergy Clin. Immun.*, 2015, 136, 441-453.